

Mikrokalorimetrische Untersuchungen zum dynamischen Verhalten von heterogenen Katalysatoren unter quasi-realen Reaktionsbedingungen

Sabine Wrabetz

Fritz-Haber-Institut der Max-Planck-Gesellschaft in Berlin



Würzburger Anwenderseminar
*Methoden der Thermischen Analyse und Rheologie
in der Entwicklung und Qualitätssicherung*
21. und 22. April 2016



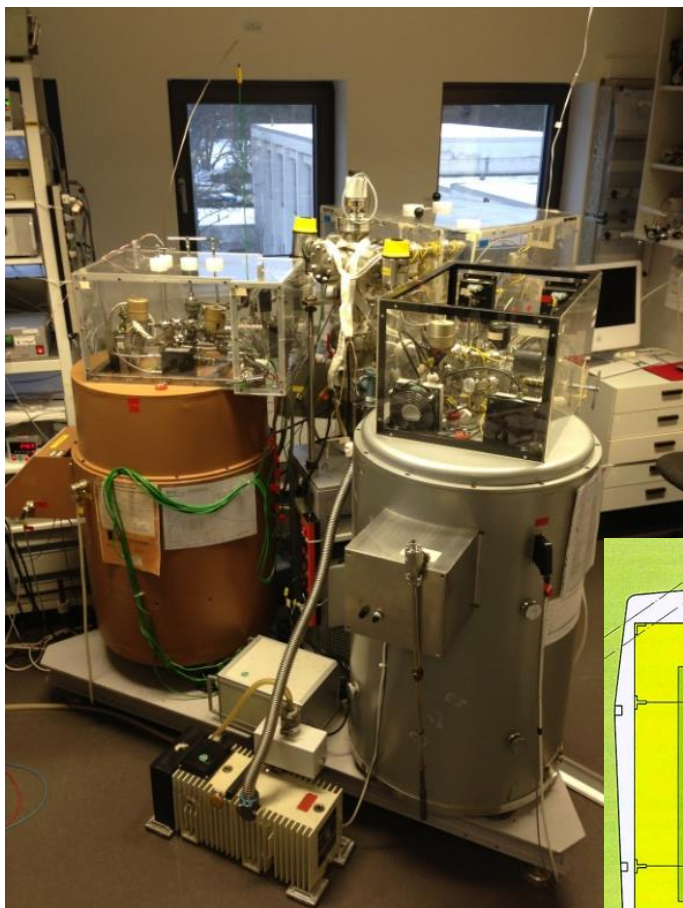
Introduction

- heterogeneous catalysis involves specific chemical interactions between the surface of a solid and the reacting gas molecules
- the catalytic cycle is generally composed of adsorption step, surface reaction processes, and desorption steps
 - 1st step in the catalytic cycle: **activation of the reacting molecules by adsorption**
(strength of chemisorption bond can effect the activation energy)
 - **adsorption phenomena** (*bond strength between adsorbate and surface*) play an important role in heterogeneous catalysis - to get a better understanding of the complex microkinetics
 - subsequent reaction and desorption processes are confirmed partially irreversible events and prove the **dynamic nature of the catalyst surface**.
→ Reactants Induced Dynamic Responses simulated *via* ads./des. cycles
- since perhaps only a minor fraction of all surface atoms form active centers

Adsorption Isothermal Microcalorimetry

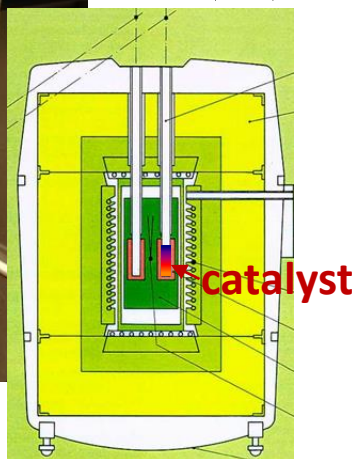
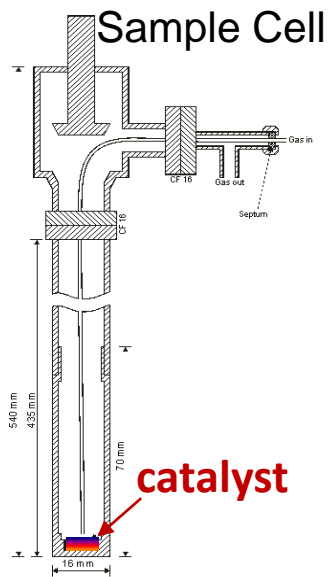
- **direct method to determine number, strength and energy distribution of the adsorption sites**
 - key to the effective use of adsorptive microcalorimetry is the **careful choice of probe molecules and the adsorption temperature** to study

Micro-calorimeters

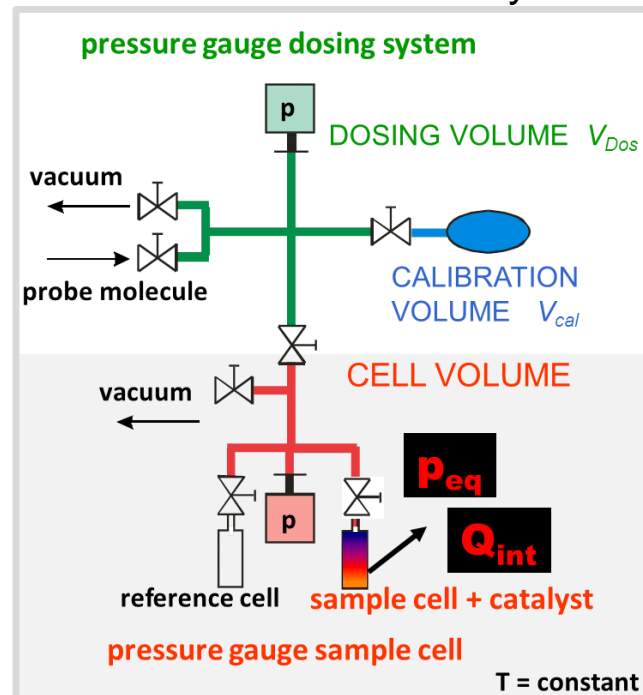


HT1000 (rt-1000°C) and **MS 70** (rt-100°C) Tian-Calvet calorimeter of SETARAM combined with a custom-designed high vacuum and gas dosing apparatus.

Karge, H.G. et al., J. Phys. Chem. 98, 1994, 8053.



Volumetric-Barometric System



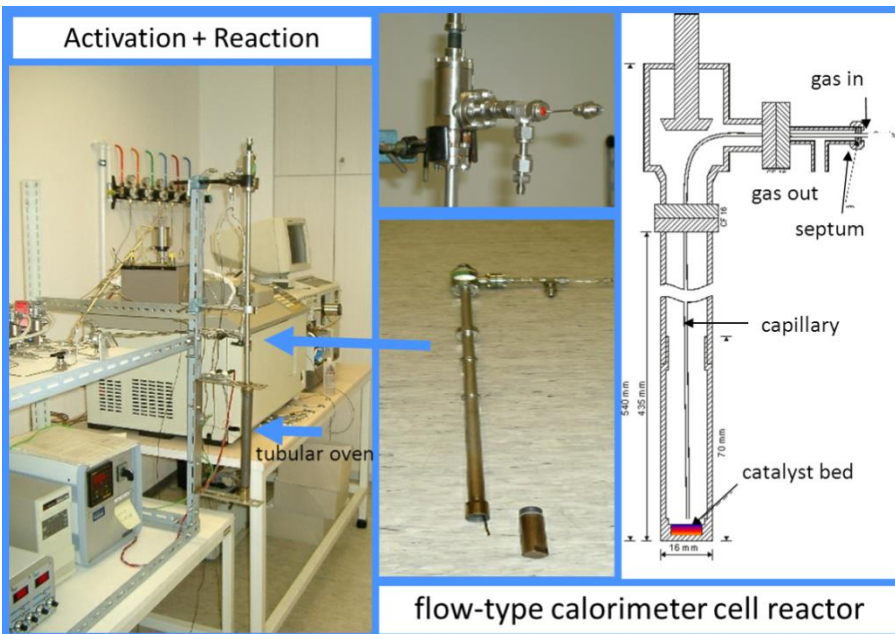
$$\Sigma n_{ads} \text{ vs } p_{eq} \quad , \quad \begin{matrix} \text{mmol} \cdot \text{g}^{-1} \\ \text{mmol} \cdot \text{m}^{-2} \end{matrix}$$

$$q_{diff} = \frac{Q_{int}}{n_{ads}} = \Delta H_{ads} \quad , \quad \text{kJ/mol}$$

$$q_{diff} \text{ vs } n_{ads} \quad , \quad \text{kJ/mol}$$

$$K = K_o \exp \frac{\Delta H_{ads}}{RT} \quad , \quad \text{hPa}^{-1}$$

$$\text{specific surface area} \quad , \quad \text{m}^2 \cdot \text{g}^{-1}$$



Activation:

UHV (10^{-8} hPa), gases (H_2 , O_2 ),
rt - $600^\circ C$

Reaction:

Calorimeter cell can be used as a flow-type reactor.

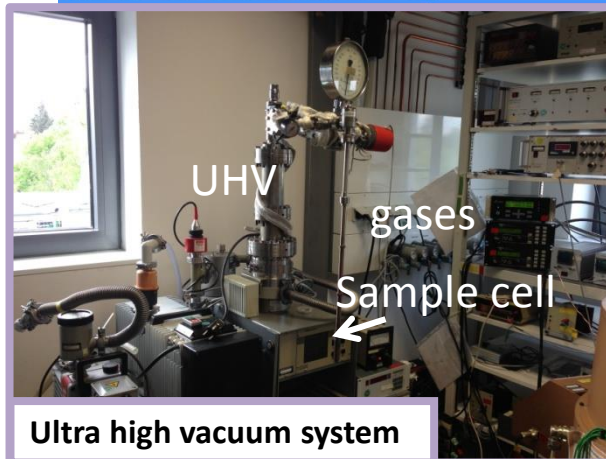
Catalyst is used in the selected reaction until steady-state performance, rt - $600^\circ C$

Transfer

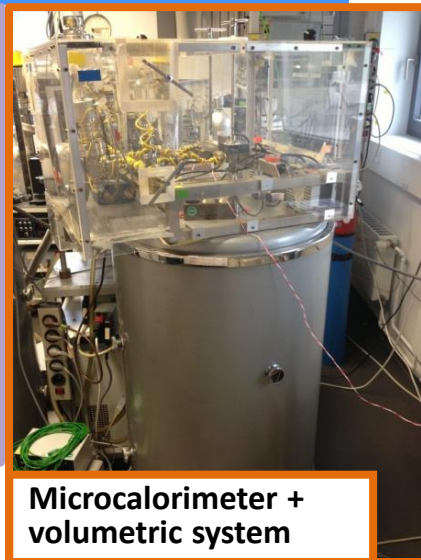
of the sample cell into the calorimeter and degassing/equilibration at T_{ads} .

Adsorptive microcalorimetric experiment:

Stepwise adsorption, desorption and re-adsorption of the selected probe molecule at the selected temperature.



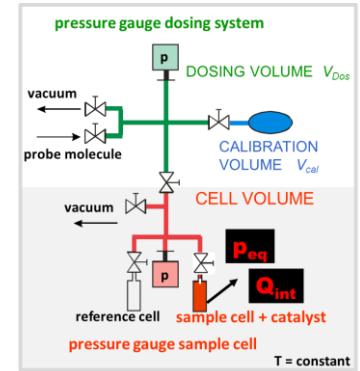
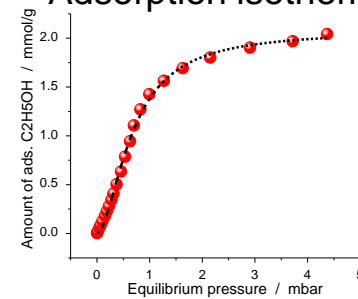
Ultra high vacuum system



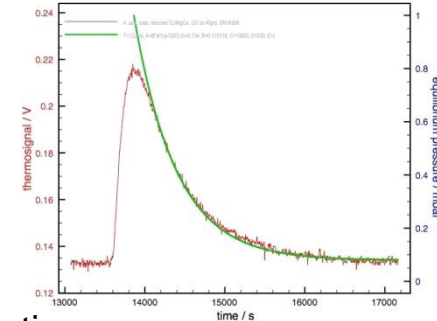
Microcalorimeter + volumetric system

- The probe molecule must be introduced **stepwise** at **constant temperature**, the pressure is increased slowly
- For each adsorption step, the **adsorbed amount** must be determined (isotherm)
- For each adsorption step, the **evolved heat** must be determined (integral heat of adsorption)
- The **differential heat** (ΔH_{ads}) can then be determined by dividing the evolved heat through the number of molecules adsorbed in a particular step

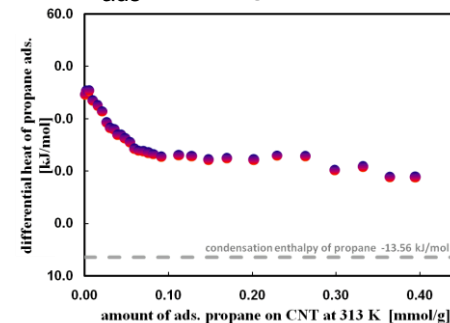
Adsorption isotherm



Integral heat of ads.

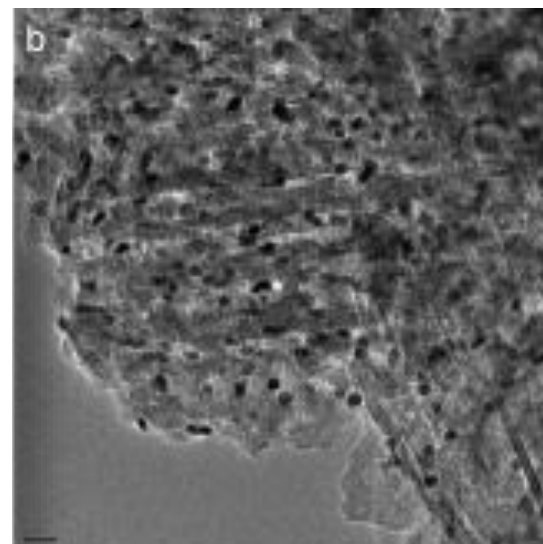


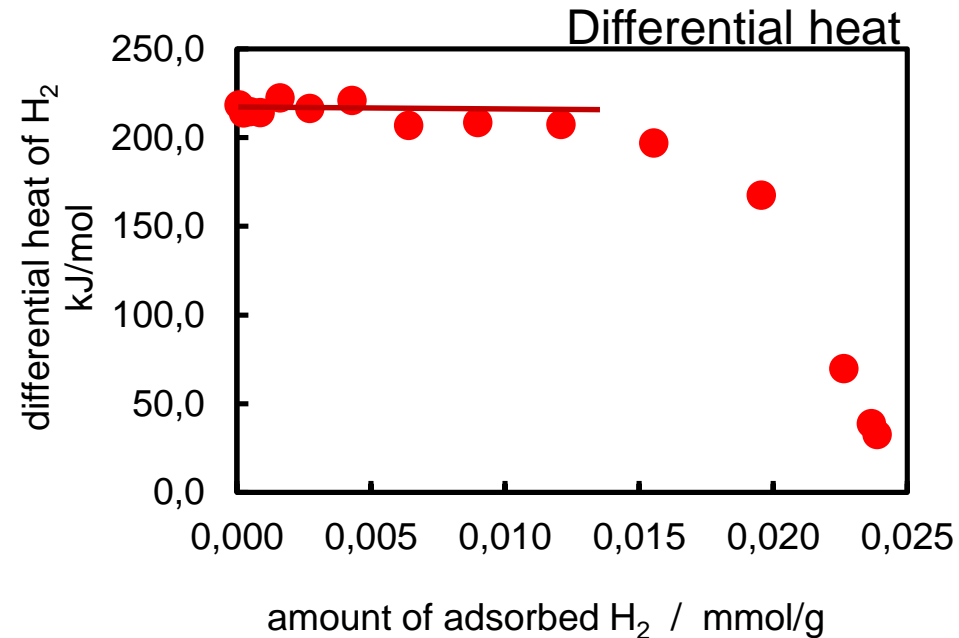
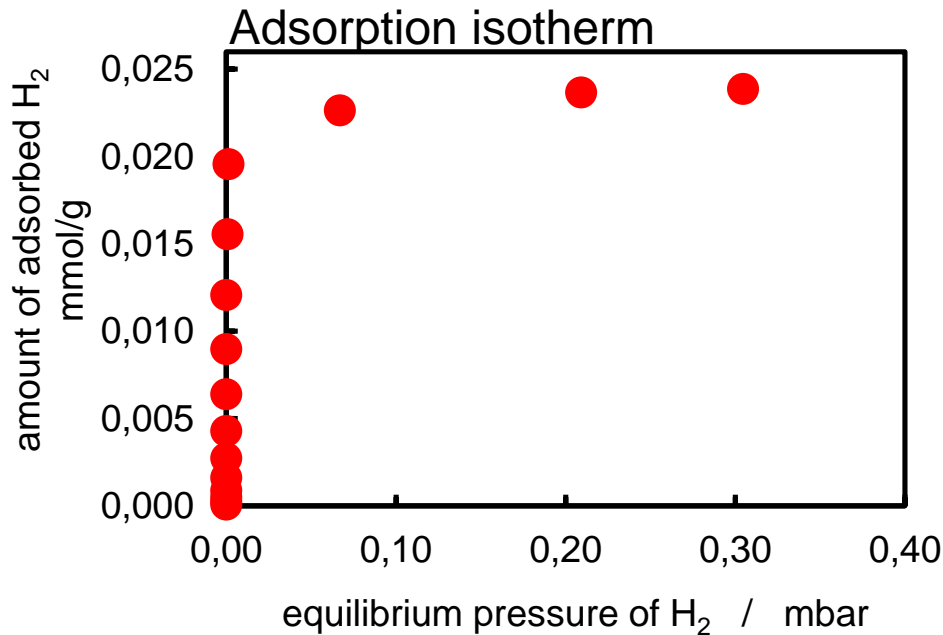
ΔH_{ads} / energy distribution



H₂ adsorption on

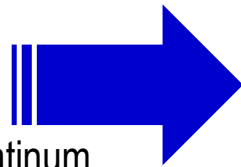
Pt_{H2-673K-2h} / **Al₂O₃** *Quantachrome Instr., Ref.-material, Cat.No.7001* **at 40°C**





Heat plateau: homogeneously distributed and **energetically uniform** adsorption sites

q_{diff} = 215 kJ/mol : chemisorption ! $\Delta_c H = 215 \text{ kJ/mol}$
 Hydrogen is dissociative adsorbed on platinum
 $\text{H}_2 + \text{Pt} + \text{Pt} \rightarrow \text{Pt-H} + \text{Pt-H} \quad \Delta_c H = 266 \text{ kJ/mol}$
 2.5% Pt/silica
 J.A. Dumesic et.al., Catal. Letters 45 (1997) 155-163.



Langmuir isotherm for dissociative adsorption

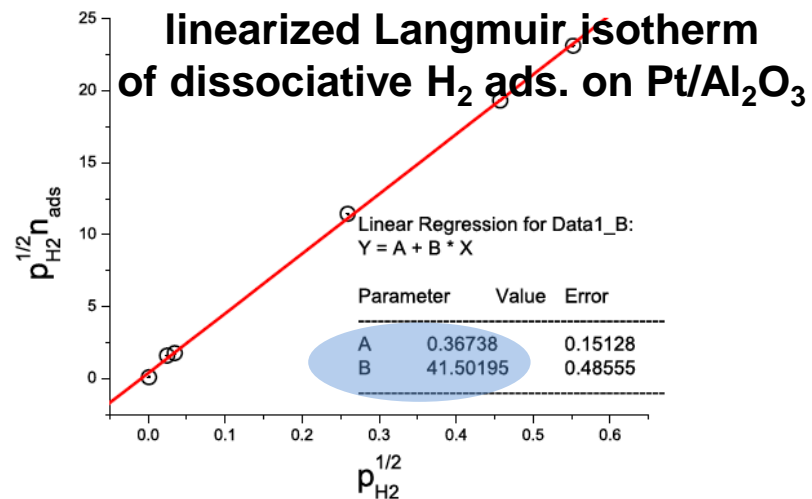
$$\theta_H = \frac{n_{ads}}{n_m} = \frac{\sqrt{pH_2 K_{ads}}}{1 + \sqrt{pH_2 K_{ads}}}$$

Linearization

$$\theta_H = \frac{n_{ads}}{n_m} = \frac{\sqrt{p_{H_2} K_{ads}}}{1 + \sqrt{p_{H_2} K_{ads}}}$$

$$n_{ads} \left(1 + \sqrt{p_{H_2} K_{ads}}\right) = n_m \sqrt{p_{H_2} K_{ads}}$$

$$\frac{1}{n_m \sqrt{K_{ads}}} + \frac{1}{n_m} \sqrt{p_{H_2}} = \frac{\sqrt{p_{H_2}}}{n_{ads}}$$



registered	$\frac{p_{H_2}}{\text{mbar}}$	10 ⁻⁶	6 · 10 ⁻⁴	1.2 · 10 ⁻³	6.69 · 10 ⁻²	2.09 · 10 ⁻¹	3.05 · 10 ⁻¹
calculated from the calibrated volumetric system	$\frac{n_{ads}}{(\text{mmol} \cdot \text{g}^{-1})}$	1.208 · 10 ⁻²	1.555 · 10 ⁻²	1.956 · 10 ⁻²	2.264 · 10 ⁻²	2.366 · 10 ⁻²	2.387 · 10 ⁻²
calculated	$\frac{\sqrt{p_{H_2}}}{\sqrt{\text{mbar}}}$	10 ⁻³	24.5 · 10 ⁻³	34.6 · 10 ⁻³	259 · 10 ⁻³	457 · 10 ⁻³	552 · 10 ⁻³
calculated	$\frac{n_{ads}}{\frac{\sqrt{\text{mbar}} \cdot \text{g}}{\text{mmol}}}$	0.083	1.58	1.77	11.44	19.32	23.13

B

$$\frac{1}{n_m} = 42 \frac{\text{g}}{\text{mmol}} \Rightarrow n_m = 24 \cdot 10^{-3} \frac{\text{mmol}}{\text{g}}$$

Specific surface area of Pt m^2_{Pt}/g_{cat}

A

$$\frac{1}{n_m \sqrt{K_{ads}}} = 0.4 \frac{\sqrt{\text{mbar}} \cdot \text{g}}{\text{mmol}} \Rightarrow K_{ads} = \left(\frac{1 \cdot \text{g} \cdot \text{mmol}}{24 \cdot 10^{-3} \text{mmol} \cdot 0.4 \sqrt{\text{mbar}} \cdot \text{g}} \right)^2$$

$$\Rightarrow K_{ads} = 10851 \text{ mbar}^{-1}$$

Specific surface area of Pt m^2_{Pt}/g_{cat}

$$S_{Pt} = \frac{n_m \cdot \text{Avogadro constant}}{\text{Surface sites density } \Gamma_{\text{fcc lattice, Pt}}}$$

$$S_{Pt} = \frac{24 \cdot 10^{-6} \text{ mol} \cdot 6.022 \cdot 10^{23} \text{ particles} \cdot \text{cm}^2}{\text{g} \cdot 1.5 \cdot 10^{15} \text{ atoms} \cdot \text{mol}}$$

$$S_{Pt} = 9667 \text{ cm}^2/\text{g} \approx 1 \text{ m}^2/\text{g}$$

$$S_{Pt}; \text{ certified by Quantachrome} = 1.146 \text{ m}^2/\text{g}$$

Final Results

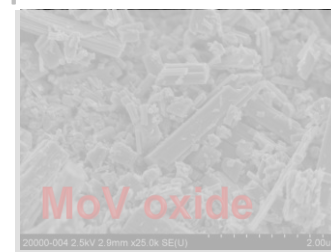
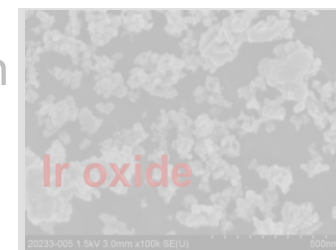
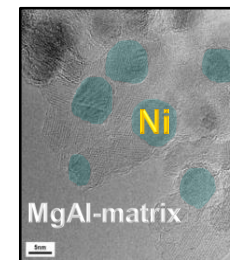
Kinetic parameters determined for the H₂ ads. on Pt/Al₂O₃

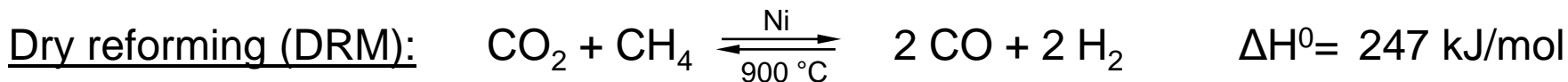
n_{mono}	=	$24 \cdot 10^{-6} \text{ mol} \cdot \text{g}^{-1}$	=	$26 \cdot 10^{-6} \text{ mol} \cdot \text{g}^{-1}$
K_{ads}	=	10851 mbar^{-1}	=	3946 mbar^{-1}
$\Delta H_{\text{ads.}}$	=	$215 \pm 4 \text{ kJ} \cdot \text{mol}^{-1}$	=	$200 \pm 4 \text{ kJ} \cdot \text{mol}^{-1}$
S_{Pt}	≈	$1.0 \text{ m}^2 \cdot \text{g}^{-1}$	≈	$1.1 \text{ m}^2 \cdot \text{g}^{-1}$

CO

Selected applications

1. Ni based catalysts for the dry reforming of methane
2. Reactive oxygen species in iridium-based oxygen evolution reaction (OER) catalysts
3. Dynamic response of a MoV oxide catalyst in propane and ethane adsorption



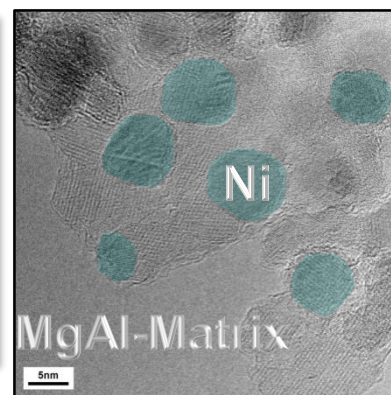
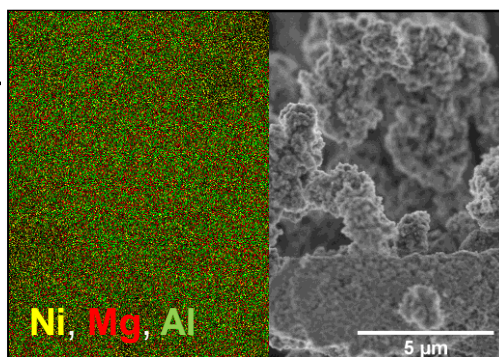


side reactions (\rightleftharpoons coking):

- Methane pyrolysis: $\text{CH}_4 \rightleftharpoons \text{C} + 2\text{H}_2$ $\Delta H^0 = 75\text{ kJ/mol}$
- Boudouard reaction: $2\text{CO} \rightleftharpoons \text{C} + \text{CO}_2$ $\Delta H^0 = -171\text{ kJ/mol}$
- reverse coal gasification: $\text{CO} + \text{H}_2 \rightleftharpoons \text{C} + \text{H}_2\text{O}$ $\Delta H^0 = -131\text{ kJ/mol}$

catalyst preparation pathway:

- synthesized by constant pH co-precipitation with Ni contents between 0 and 55 wt.-%.
- decomposition to mixed oxides by calcination at 600°C



The catalyst:

Ni/MgAl oxide

by reduction at 1000°C

- $d_{\text{P, Ni}} = 7 - 20\text{ nm}$ in all samples

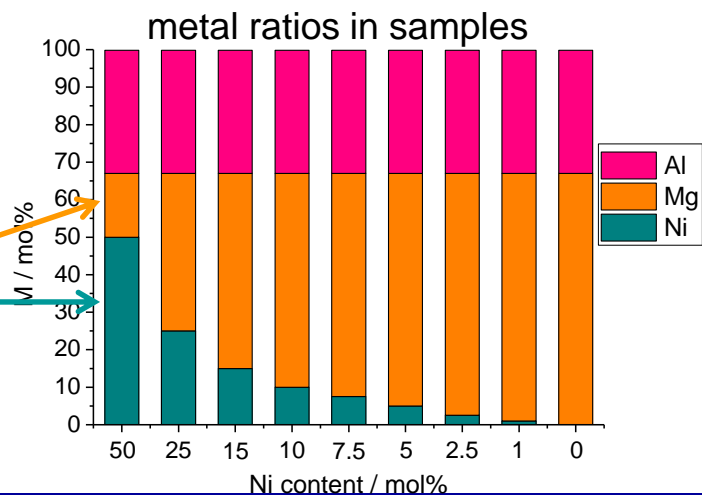
Ni/MgAl oxide catalysts:

- 0-55 wt.-% Ni

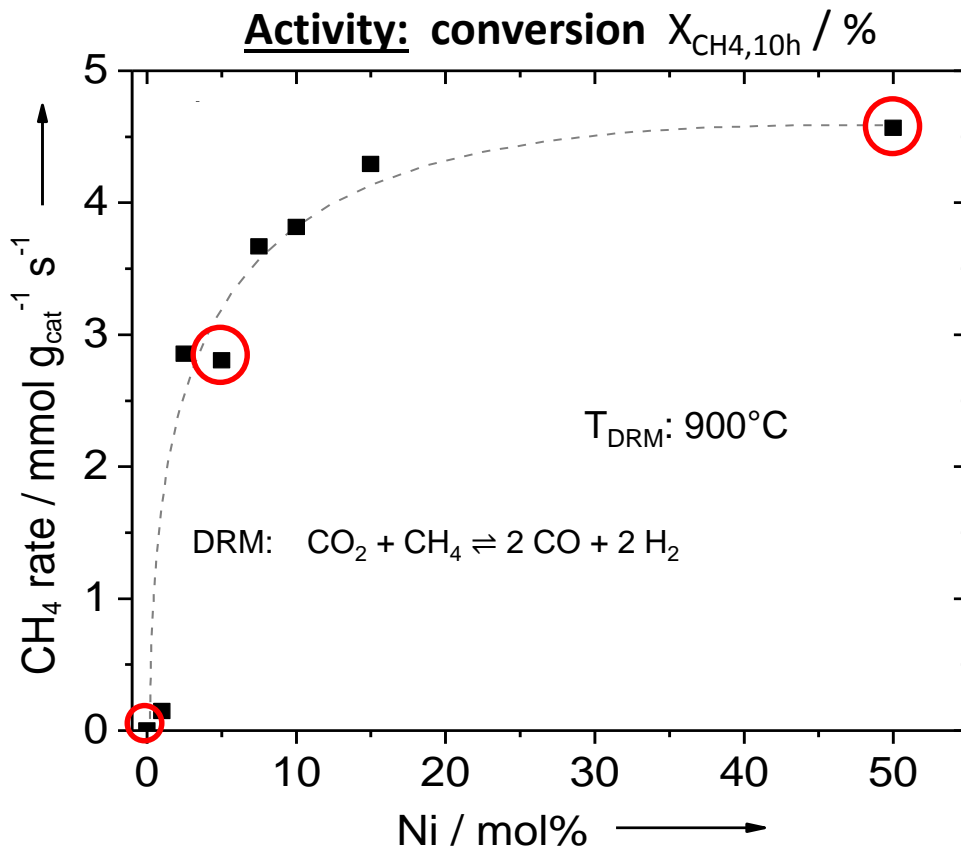
50 mol% Ni: Mg : Al = 1:2 (spinel stoichiometry)

XRD: metallic Ni in spinel matrix (+ MgO)

< 50 mol% Ni: excess of Mg



Intention: In order to define a **structure-activity-relationship**, the properties of the Ni based catalyst were studied by adsorption microcalorimetry using **CO (product) at 30°C**.²



Sample	$X_{\text{CH}_4,10\text{h}} / \%$
Ni50	73
Ni15	68
Ni10	61
Ni7.5	59
Ni5	50
Ni2.5	46
Ni1	3
Ni0	0

- free Ni sites are essential
- relationship is not linear
- structure sensitivity¹

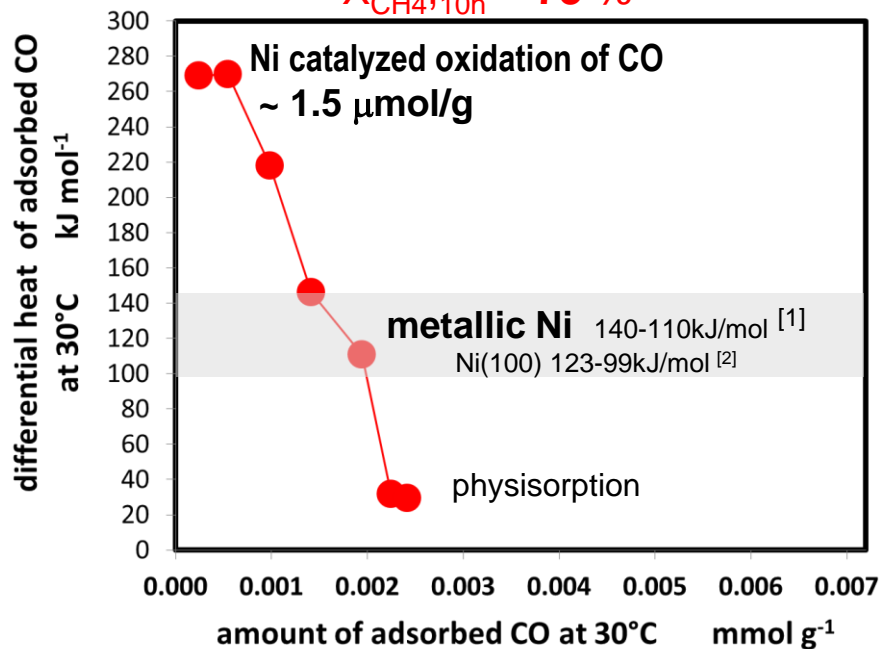
¹ J. Wei, E. Iglesia, *J. Phys. Chem. B* **2004**, 108, 4094-4103.

² M. Mette,S. Wrabetz.....M. Behrens, submitted Dec. 2015.

Microcalorimetry CO at 30°C

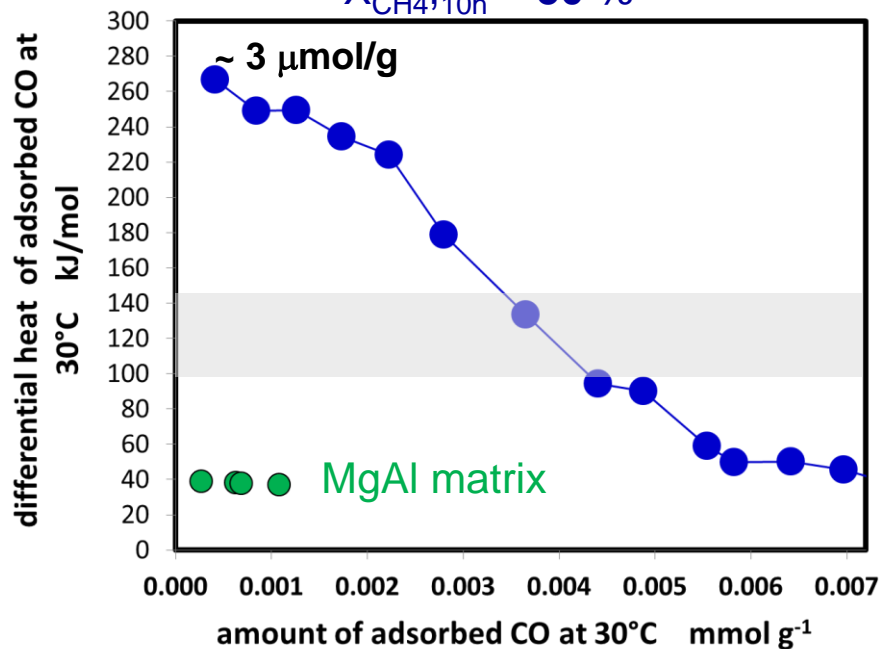
50mol% Ni/MgAl oxide

$X_{\text{CH}_4, 10\text{h}} = 73\%$



5 mol% Ni/MgAl oxide

$X_{\text{CH}_4, 10\text{h}} = 50\%$



- $\Delta n \sim 4\mu\text{mol/g}$
- ~ 270 kJ/mol: Ni catalyzed oxidation reactions of CO with the oxidic matrix are more pronounced for the catalyst with less Ni and therefore a higher MgO content in the oxidic matrix.

[1] A. Tanksale, J.N. Beltramini, J.A. Dumesic, G.Q. Lu, *Journal of Catalysis* 258 (2008) 366–377.

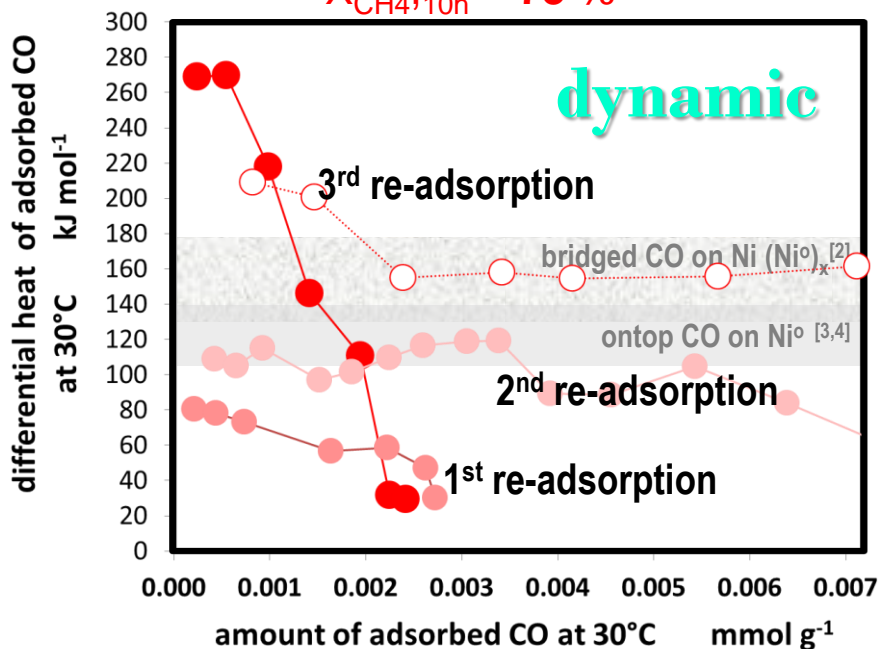
[2] J. T. Stuckless, N. Al-Sarraf, C. Wartnaby, D. A. King, *J. Chem. Phys.* **1993**, 99, 2202-2212.

M. Mette, S. Wrabetz, M. Behrens, R. Schlögl et al., submitted Jan 2015.

Microcalorimetry Adsorption/Desorption cycles

50mol% Ni/MgAl oxide

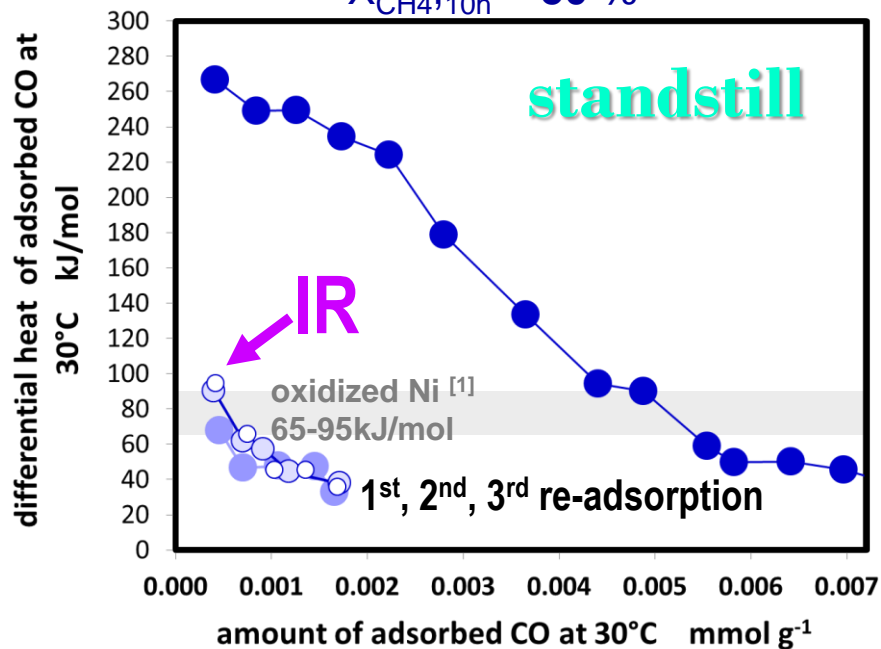
$X_{\text{CH}_4, 10\text{h}} = 73\%$



CO at 30°C

5 mol% Ni/MgAl oxide

$X_{\text{CH}_4, 10\text{h}} = 50\%$



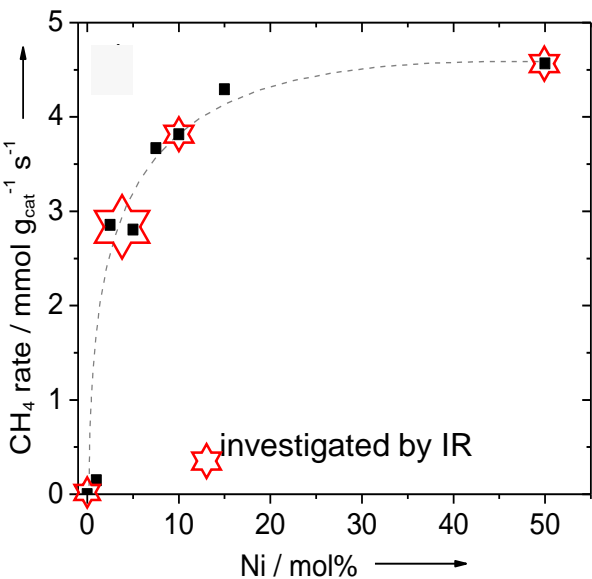
- The mobile character of the Ni-based adsorption sites of the most active surface is apparently favorable for the catalytic performance; perhaps because of generation and/or regeneration of the used active sites.

[1] M. Cerro-Alarcó, B. Bachiller-Baeza, A. Guerrero-Ruiz, I. Rodríguez-Ramos, *J. Mol. Catal. Chem.* 2006, 258, 221-230.

[2] R. S. Bordoli, J. C. Vickerman, J. Wolstenholme, *Surf. Sci.* 1979, 85, 244-262.

[3] A. Tanksale, J.N. Beltramini, J.A. Dumesic, G.Q. Lu, *J. of Catalysis* 258 (2008) 366-377.

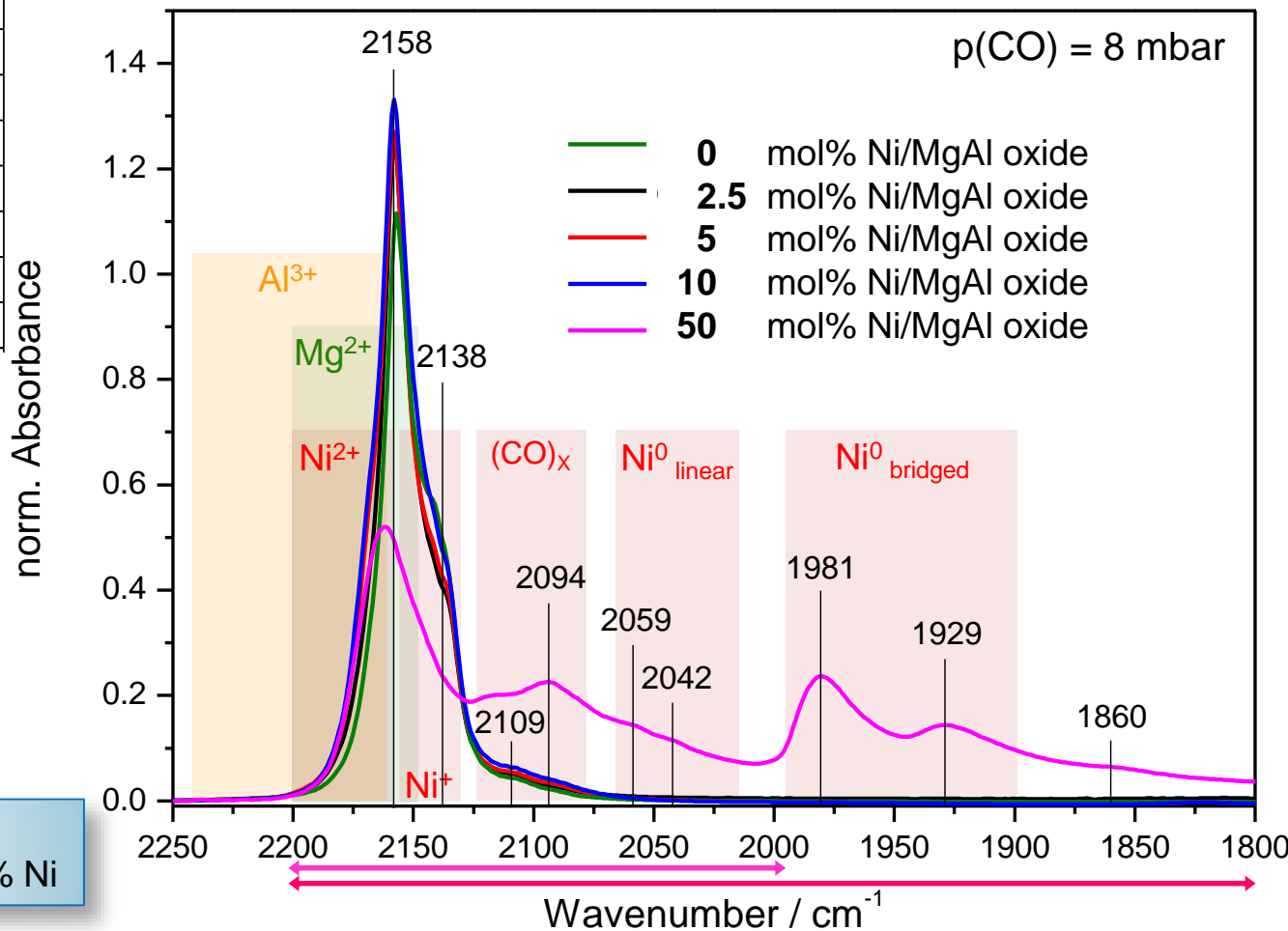
[4] J. T. Stuckless, N. Al-Sarraf, C. Wartnaby, D. A. King, *J. Chem. Phys.* 1993, 99, 2202-2212.
M. Mette, S. Wrabetz, M. Behrens, submitted Jan 2015.



- spectra of CO adsorbed on NiMgAl samples taken at full CO coverage
- reference band positions taken from literature [1]

- metallic Ni sites in Ni50 only
- mainly cationic Ni in <50mol% Ni

FTIR spectroscopy CO adsorption at 77K



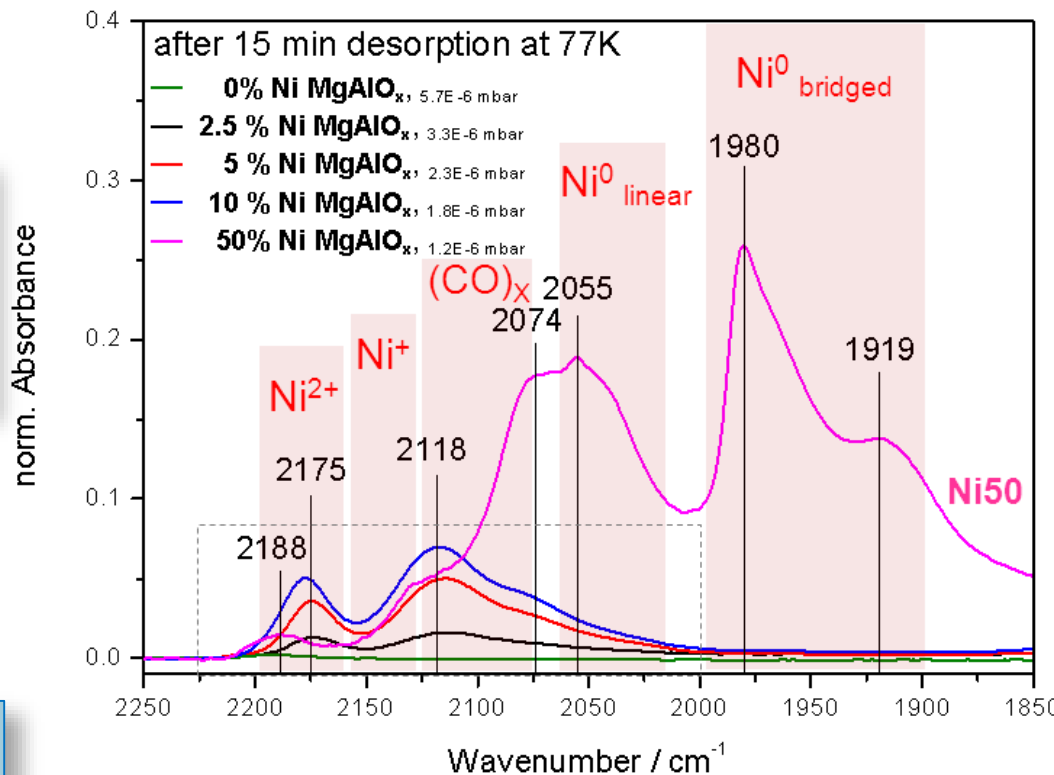
[1] K. I. Hadjiivanov, G. N. Vayssilov, *Adv. Catal.* **2002**, 47, 307-511

spectra after evacuation

- amount of residual CO ads. complexes correlates with Ni content
- Ni⁰ agglomerates in Ni50 sample
- some isolated Ni⁰ sites also in 2.5-10% Ni
- mainly Ni^{x+} in 2.5-10% Ni

➤ **Results correlates very well with the calorimetric observations**

CO desorption at 77K on Ni MgAlO_x



weak interaction	stronger interaction
oxidized Ni	metallic Ni
65-95kJ/mol	140-110kJ/mol
	Ni(100) 123-99kJ/mol

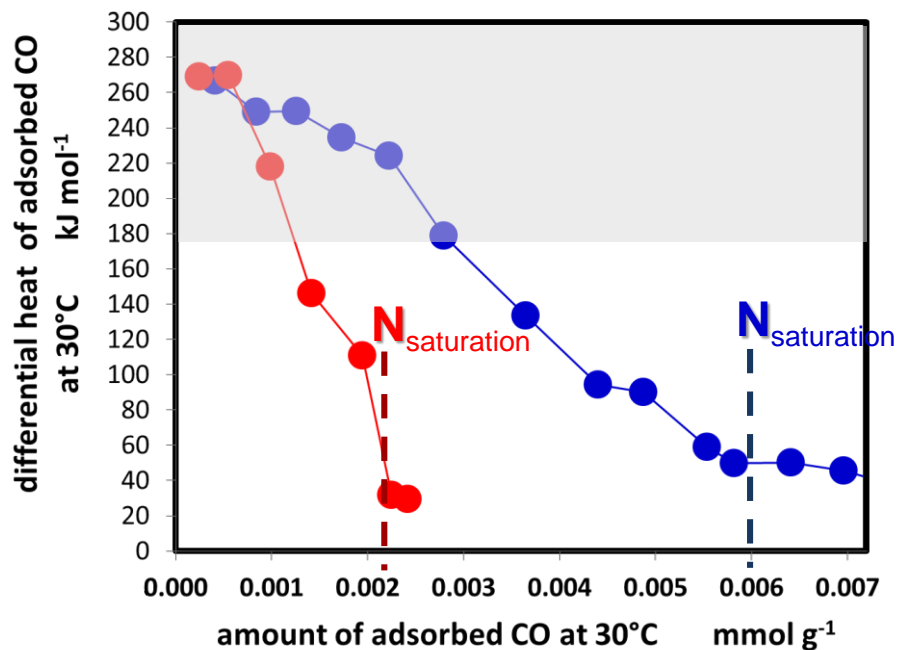
50mol% Ni/MgAl oxide

$X_{\text{CH}_4, 10\text{h}} = 73\%$

5 mol% Ni/MgAl oxide

$X_{\text{CH}_4, 10\text{h}} = 50\%$

Metal surface area of Ni for CO at 30°C



$S_{\text{Ni-CO}} = 0.09 \text{ m}^2/\text{g}$

$S_{\text{Ni-BET-Calc., N}_2\text{-77K}} = 226 \text{ m}^2/\text{g}$

$S_{\text{Ni-H}_2\text{-TPR}} = 6 \text{ m}^2/\text{g}$

$S_{\text{Ni-CO}} = 0.24 \text{ m}^2/\text{g}$

$S_{\text{Ni-BET-Calc., N}_2\text{-77K}} = 205 \text{ m}^2/\text{g}$

$S_{\text{Ni-H}_2\text{-TPR}} = 3 \text{ m}^2/\text{g}$

$$\begin{aligned}
 S_{\text{Ni, CO, 30grd}} &= N_{\text{saturation}} \cdot \text{stoichiometric factor} \cdot \text{Avogadro's number} \cdot \text{atomic cross section of the metal} \\
 &= 2.2 / 6 \cdot 10^{-6} \text{ mol} \cdot 1 \cdot 6.023 \cdot 10^{23} \cdot 0.0649 \cdot 10^{-18} \text{ m}^2 \\
 &= 0.086 / 0.235 \text{ m}^2/\text{g}
 \end{aligned}$$

Ni based catalysts for the dry reforming of methane

➤ The most active catalyst is characterized by:

- big Ni⁰ agglomerates
- in the presence of CO an additional notable amount of Ni⁰ is formed
- dynamic character of the Ni-based adsorption sites
- relatively low amount of Ni free or slightly affected MgAl-matrix and hence less degree of oxidation of CO
- relatively small amount of cationic Ni

$$d_{P, TEM} = 19.4 \pm 7.1 \text{ nm}$$
$$n_{Ni^0} \sim 5 - 7 \text{ } \mu\text{mol /g}$$
$$q_{diff} = 170 - 110 \text{ kJ/mol}$$

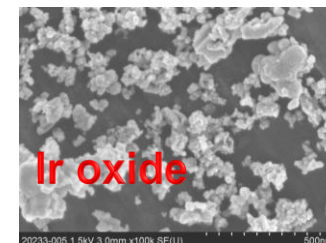
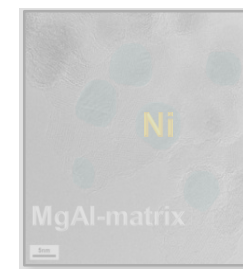
$$n_{matrix} \sim 1.5 \text{ } \mu\text{mol /g}$$
$$q_{diff} = 270 - 170 \text{ kJ/mol}$$
$$n_{Ni^{x+}} \sim 1 - 2 \text{ } \mu\text{mol /g}$$

➤ Catalytic aspect:

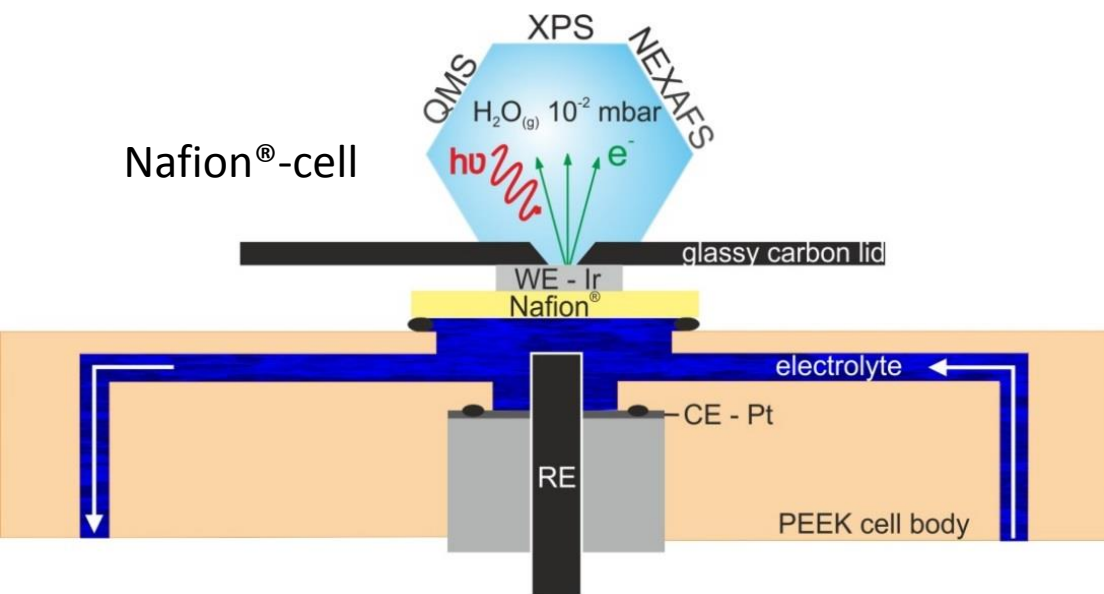
- The ***mobile character of the Ni-based adsorption sites*** of the most active surface is apparently favorable for the catalytic performance; perhaps because of generation and/or regeneration of the used active sites.

Selected applications

1. Ni based catalysts for the dry reforming of methane
2. Reactive oxygen species in iridium-based oxygen evolution reaction (OER) catalysts
3. Dynamic response of a MoV oxide catalyst in propane and ethane adsorption



Ir-based catalysts are promising materials to electrocatalyze the oxygen evolution reaction (OER) in acidic media.



XPS in-situ cell is operated at BESSY

Aim:

→ Monitor changes in the electronic structure during the oxygen evolution reaction (OER)

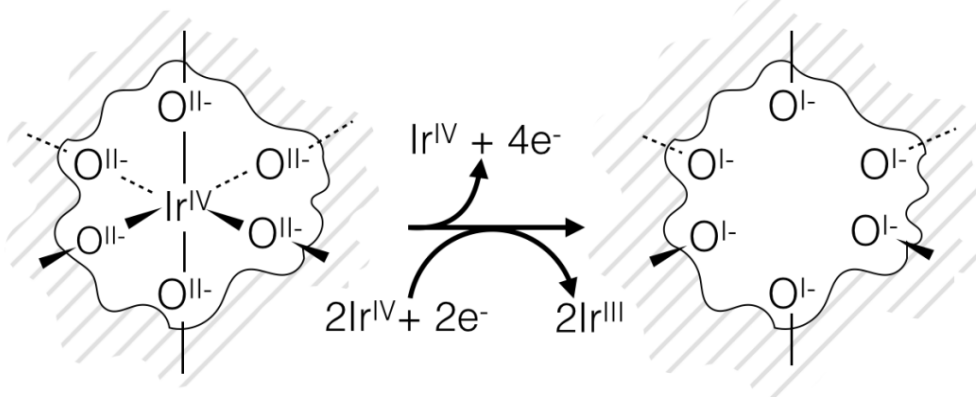
Note:

- X-rayNear Edge X-ray Absorption Fine Structure (NEXAFS)
- photoelectron spectroscopy (XPS)
- The FHI high pressure XPS set-up is operated at BESSY (Berliner Elektronenspeicherring-Gesellschaft für Synchrotronstrahlung m.b.H.)

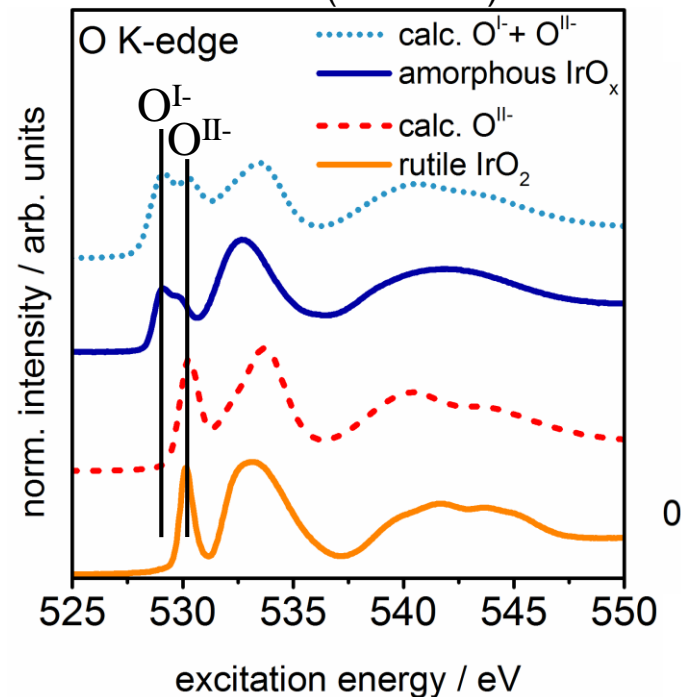
→ We expect the formally $O^{\cdot-}$ species contained in IrO_x as an active site in the OER

- Catalyst:
- amorphous $Ir^{III/IV}$ oxyhydroxides (IrO_x)
 - crystalline rutile-type IrO_2

Defect model for iridium oxide



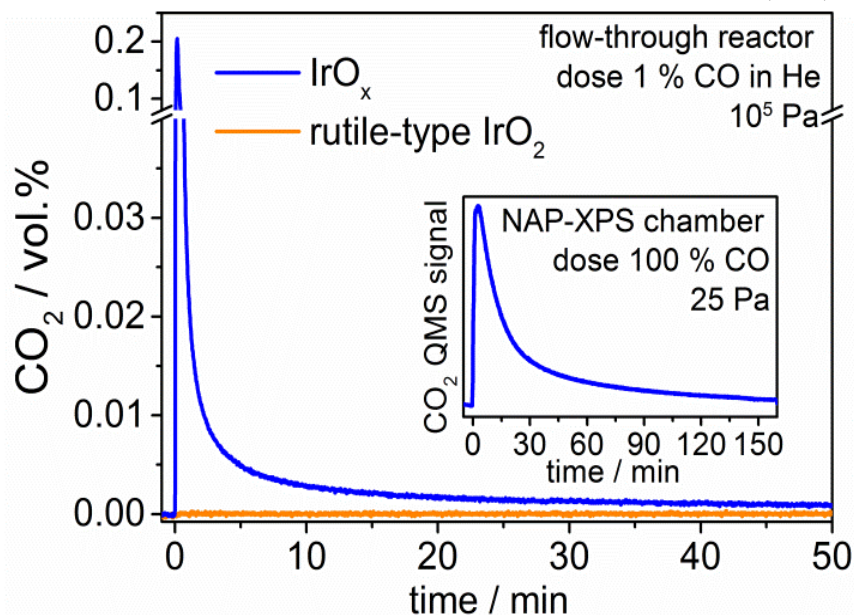
X-ray Near Edge X-ray Absorption Fine Structure (NEXAFS)



↳ We use **CO titration** as a prototype chemical probe reaction to investigate the reactivity of active oxygen species



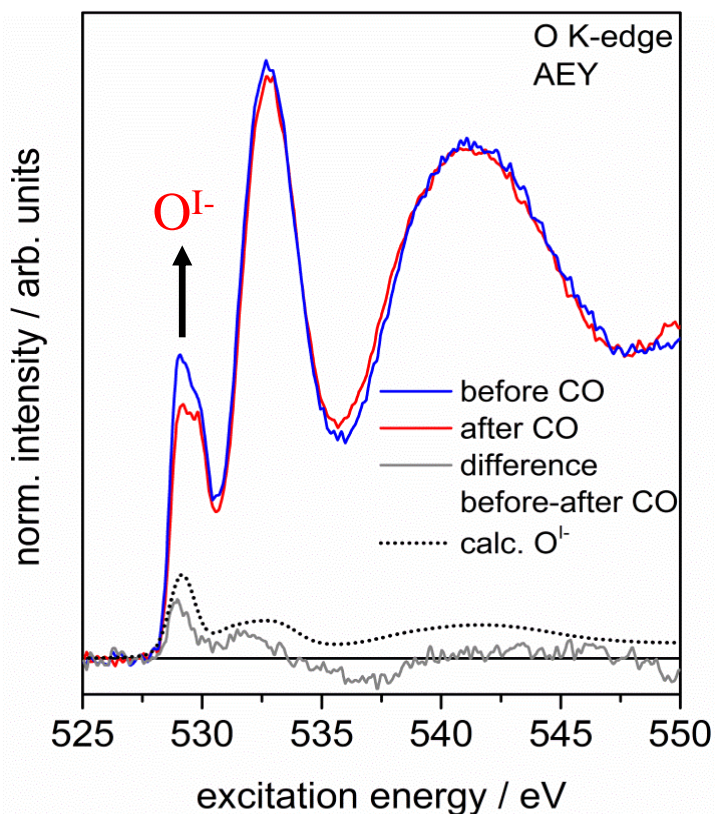
CO₂ concentration in effluent gas stream over time after CO is introduced (r.t.)



The higher level of activity for the OER of X-ray amorphous Ir^{III/IV} oxyhydroxides (IrO_x) as compared to crystalline rutile-type IrO₂ may be connected to **more active oxygen species** present in IrO_x.

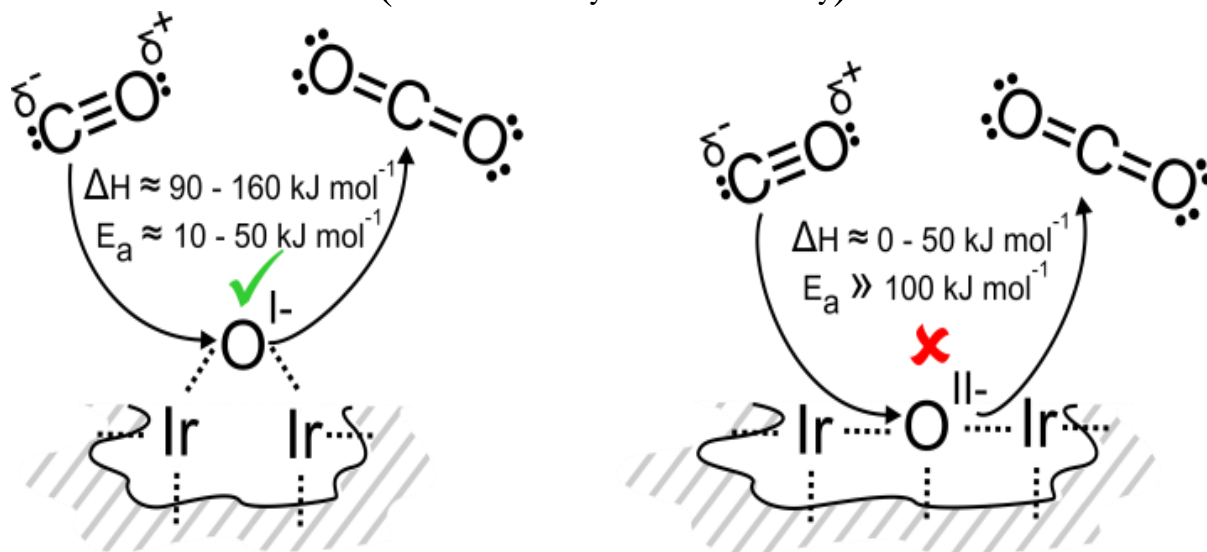
- To test this hypothesis “*O^{I-} species the active site*”, we employ XPS and NEXAFS and monitor the regions characteristic for the O^{I-} species (~529 eV).

Comparison of our theoretical and experimental O K-edge spectra



- only IrO_x contains a large abundance of formally **O^{I-} species**,
 - the difference spectrum shows the considerable decrease of the **529 eV** feature
- this **O^{I-}** type of oxygen is a likely candidate for the oxygen active in CO oxidation

Calculated activation barrier (E_a) and reaction enthalpies (ΔH)
(DFT Density functional theory)



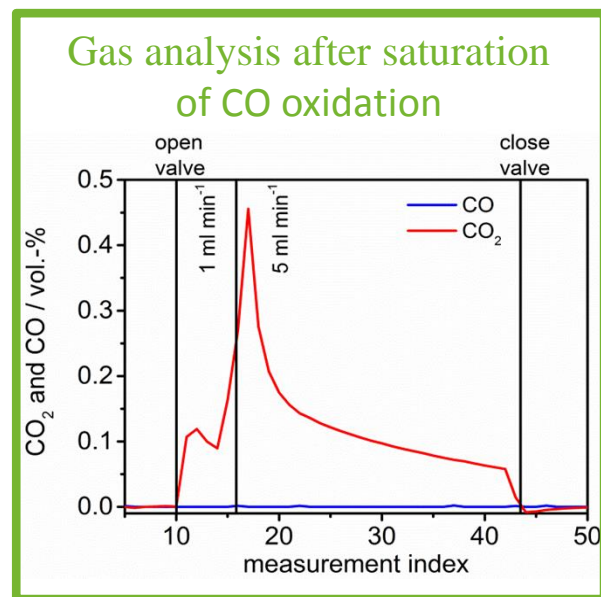
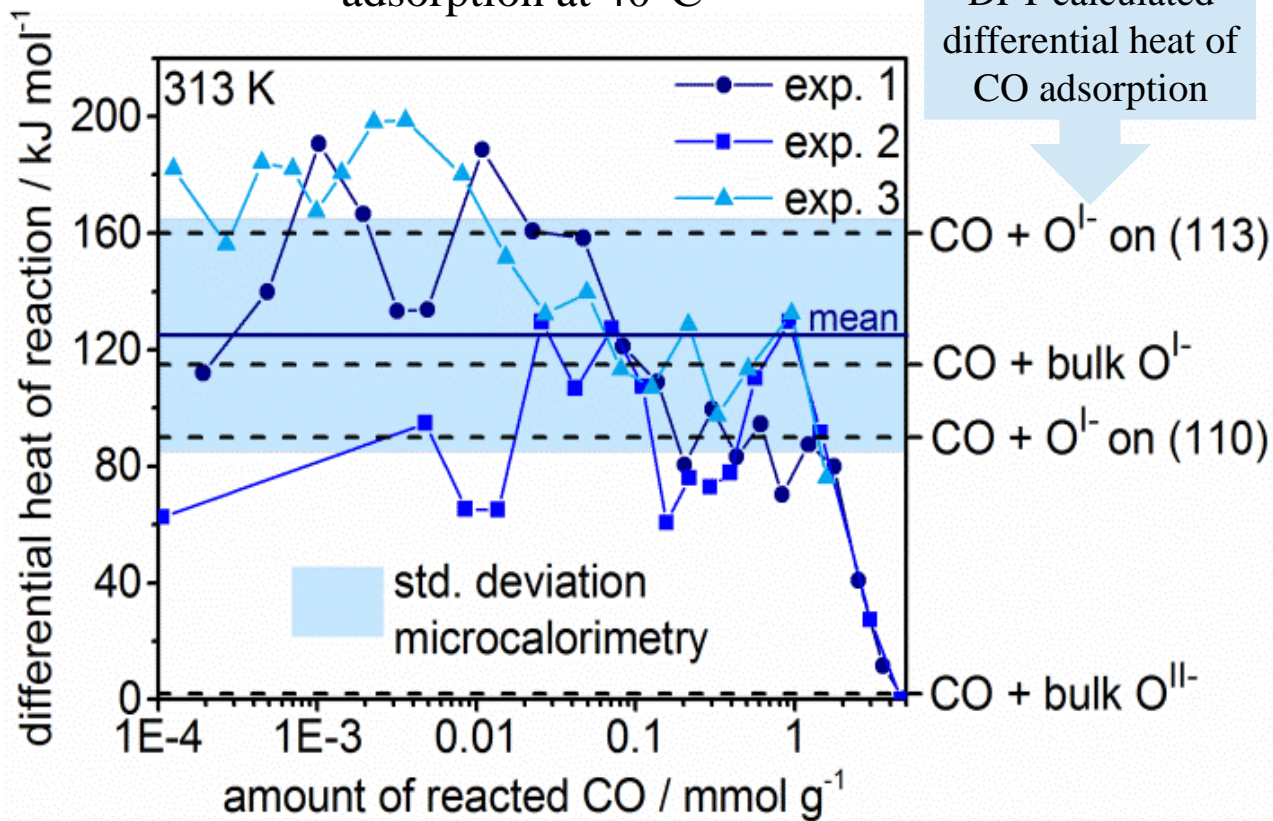
RT

The schemes summarize the CO titration of different oxygen species on iridium oxide surfaces with respect to their **calculated activation barrier and reaction enthalpies**.

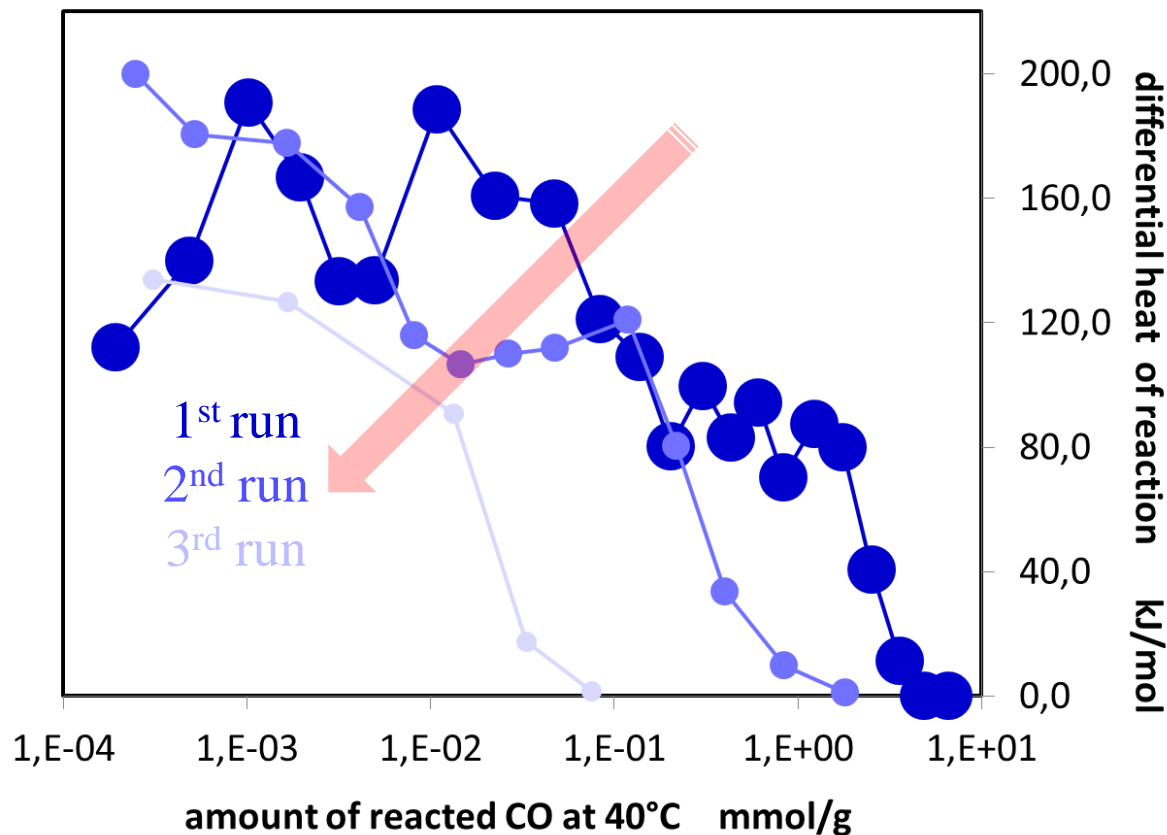
Energetically, the reaction of CO with O^{I-} seems feasible, while the reaction with O^{II-} seems not possible to take place at room temperature.

Microcalorimetry – the corresponding experiment

Differential heat of CO adsorption at 40°C



.....monitored by CO adsorption-desorption cycles



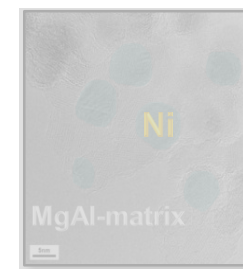
→ Irreversible consumption of active O⁻ sites

Regeneration of active O⁻ species by ozone treatment

- Our experiments outline a facile chemical probe reaction for active oxygen species on Ir-based OER catalysts.
- ✓ Ab initio calculations combined with microcalorimetry confirmed that these defective O^{1-} species may act as sacrificial oxygen in a stoichiometric reaction with CO to form CO_2 .
- ✓ XPS and XAS, revealing that electrophilic O^{1-} species were consumed in this process
- ✓ Adsorption-desorption cycles of CO using microcalorimetry show the dynamic character of the catalyst and confirmed the consumption of active sites.
- ➔ These observations explain the increased OER activity (r.t.) of amorphous IrOx structures containing such electronic defects in the anionic framework when compared to stoichiometric rutile-type IrO_2 lacking such defects.

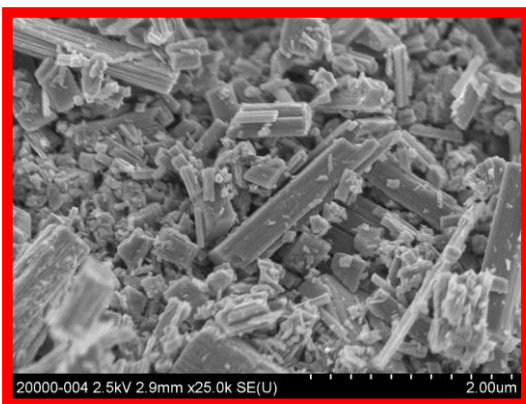
Selected applications

1. Ni based catalysts for the dry reforming of methane
2. Reactive oxygen species in iridium-based oxygen evolution reaction (OER) catalysts
3. Dynamic response of a MoV oxide catalyst in propane and ethane adsorption

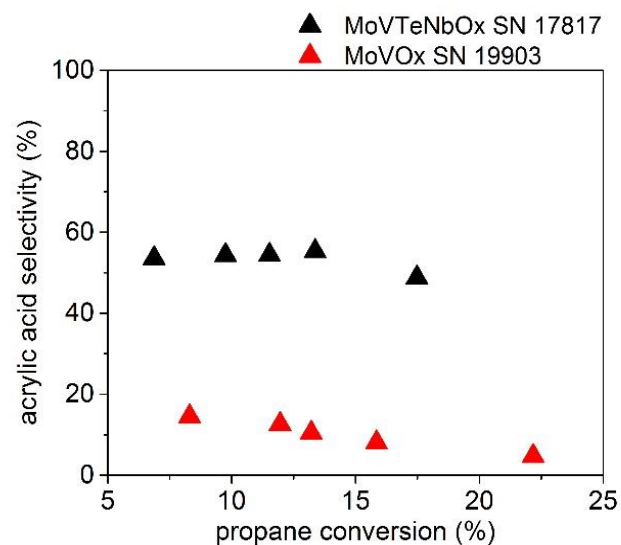


MoV oxide #20000

- Synthesis: hydrothermal method and subsequent washing procedure [1]
- Structure: M1
- Selectivity to acrylic acid: $S_{aa} = 5-10\text{mol-}\%$
- BET = $25.52\text{ m}^2/\text{g}$
- Particle size: multimodale distribution



Low selectivity of MoV oxide in oxidation of propane to acrylic acid.



MoV oxide, which is a versatile oxidation catalyst in liquid-phase oxidation reactions or in the oxidative dehydrogenation of ethane.

In contrast



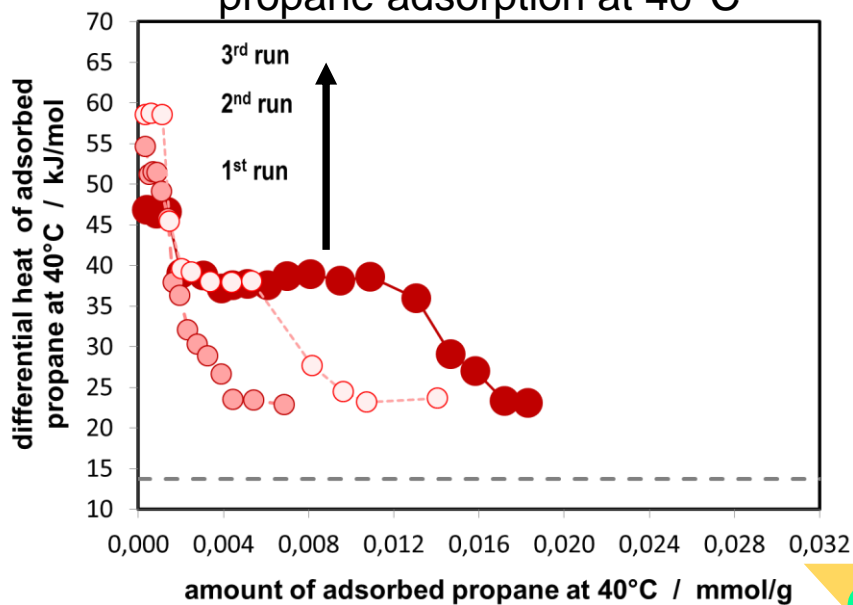
Dynamic response of a MoV oxide catalyst in propane and ethane adsorption



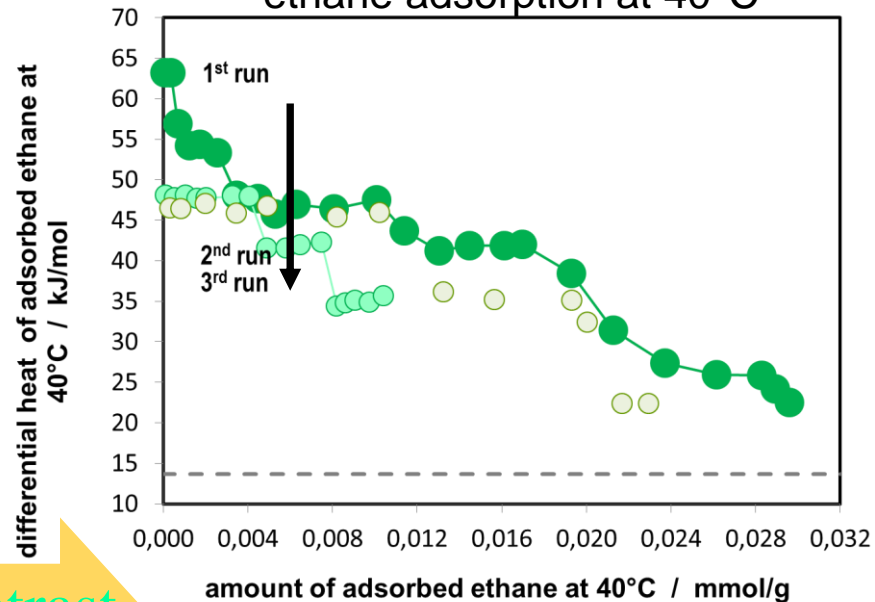
We favor on the study of adsorption-desorption cycles which can give new insights into the dynamic behavior of the catalyst surface.

Dynamic response of the catalyst to the reactants
PROPANE and ETHANE as an indicator of activity !

Differential heat of propane adsorption at 40°C



Differential heat of ethane adsorption at 40°C



Contrast

- re-adsorption of propane reveals a drastic reduction of the adsorption capacity and the formation of energetically stronger adsorption sites at r.t.
- $S_{\text{specific for propane}} \sim 3.6 \text{ m}^2/\text{g}$

- ethane interacts relatively strong 65 kJ/mol with the surface adsorption sites of MoV oxide
- adsorption enthalpy as well as the number of adsorption sites is reduced during the second cycle. Further adsorption-desorption cycles cause no change.
- $S_{\text{specific for ethane}} \sim 2.9 \text{ m}^2/\text{g}$

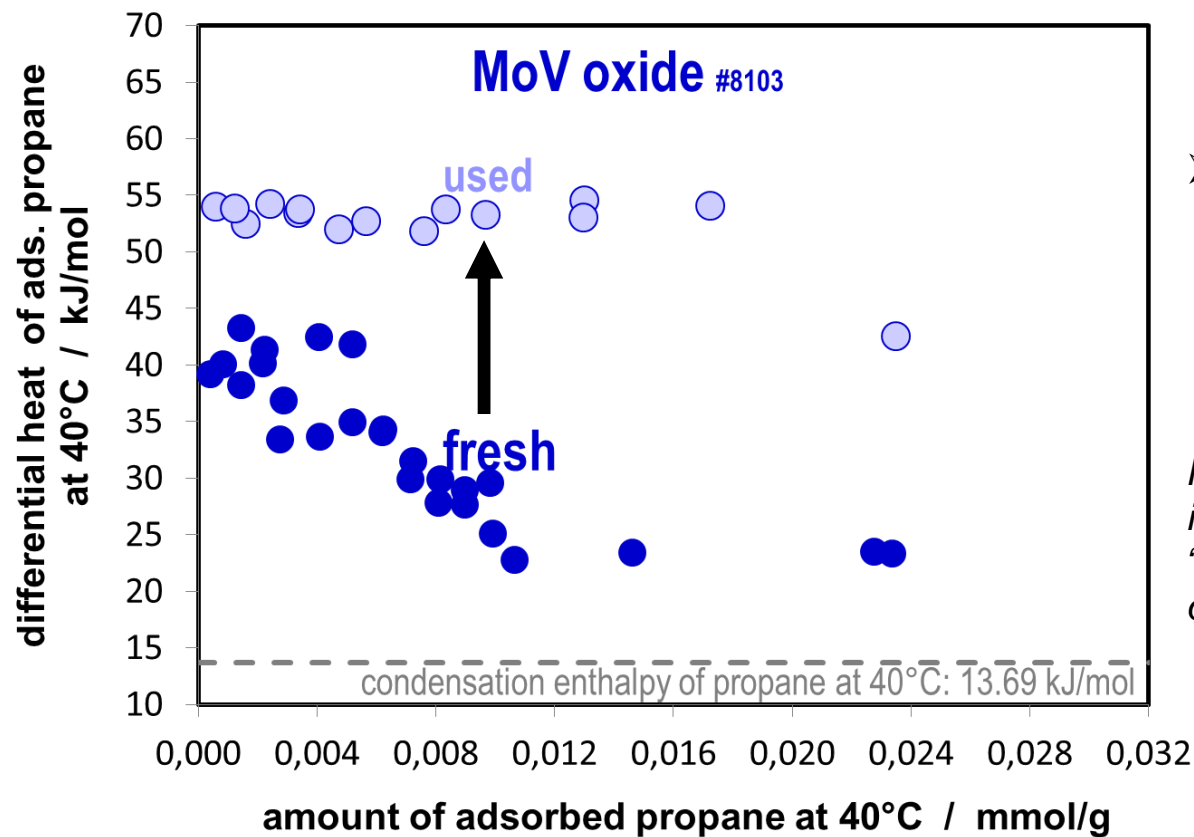
$$S_{\text{e.g. MoV oxide}} = n_{\text{ads.}} \cdot \text{Avogadro const.} \cdot S_{1:1, \text{ assumed}} \cdot \text{cross-section area}$$

39Å² for propane
22Å² for ethane

Surface dynamics studied *in situ*

in agreement

Surface dynamics studied *ex situ*



- Formation of energetically stronger surface adsorption sites for propane during oxidation reaction of propane.

Note: The MoV oxide catalyst was investigated in the prepared state “fresh” and post-reaction state “used” of the surface.



Dynamic response of a MoV oxide catalyst in propane and ethane adsorption



MAX-PLANCK-GESELLSCHAFT

- **different behavior** of different educts on the surface of the MoV oxide catalyst
- **The low selectivity** of the MoV oxide in propane oxidation may be attributed to the **dynamic generation** of strong adsorption sites provoked by the reactant itself.
- *in situ* and *ex situ* studies reveal the same trend



Thank you for your attention



<http://www.fhi-berlin.mpg.de>

Dept. of Inorganic Chemistry, Director: Prof. R. Schlögl

